Finite element simulations of drop indentations into oily clay

Dennis Bo Rahbek

FFI Forsvarets
forskningsinstitutt

Finite element simulations of drop indentations into oily clay

Dennis Bo Rahbek

Keywords

Lette beskyttelsesmaterialer

Ballistisk leire

Numerisk simulering

IMPETUS Afea

Materialmodell

Approved by

Rune Lausund	Project manager
Svein Rollvik	Director of Research
Jon E. Skjervold	Director

English summary

When testing equipment for personnel protection a set of requirements usually has to be followed. One of the most common sets of test requirements is set by the American National Institute of Justice 0101.06 standard. Among the conditions are a list of requirements for the ballistic clay, Roma Plastilina no. 1, used as backing for the test specimens. The clay has to be tested in a ball drop test, both before and after being used for tests on the personnel protection equipment. In ballistic tests at Forsvarets forskningsinstitutt, an oily Roma Plastilina type clay is often used as backing material, which makes a better understanding of the clay behaviour highly relevant. Unfortunately, very little work on the clay is found in literature.

In order to study the ballistic clay used at Forsvarets forskningsinstitutt, a set of ball drop tests have been conducted. The impact of the steel ball with the clay was monitored with a high speed camera to allow the penetration dynamics to be studied. These experimental results were used as reference points for a set of numerical studies. The Finite Element Method in the IMPETUS Afea software package, was used to test if it would be possible to simulate the ball drop test reliably. The simulations were initially performed with a simple model for the clay, and step by step the influence of various parameters were studied. In this manner, relevant parameters and additions and changes to the material model could be found.

The simulations showed that the initial and simple model with a linear yield stress curve for the clay, was not adequate to model the penetration dynamics. The steel ball and clay showed too heavy oscillations after impact in the simulations with this model. Other and slightly more complex yield stress curves were tested, however, only with minor improvements in the results. In order to lower the oscillatory behaviour after impact, damping terms were introduced to the clay material model. This resulted in less oscillations, but the experimental results could not be reproduced acceptably. However, when the clay was tried modelled by a visco-plastic material model with built in damping, the behaviour of the clay in simulations reproduced the experimental results satisfactorily.

With the proper parameters, simulations with the visco-plastic model give reasonable results within the strain rate, temperatures and level of plasticity observed in the experimental tests. The model is expected to be adequate for use in more complex simulations on impact of hard core projectiles on hard ceramic, since the uncertainties in the models for ceramic and the hard projectile core are rather large. However, further work on the clay model would be needed if this model is going to be used in simulations where the clay has a larger influence on the dynamics. Though for now, the present result is sufficient.

Sammendrag

Under test av utstyr til personlig beskyttelse er det vanligvis en rekke krav som skal overholdes. En av de mest alminnelige testspesifikasjonene er utarbeidet av Amerikanske National Institute of Justice og finnes i 0101.06 standarden. I denne finnes en rekke krav til blant annet den leiren som benyttes som bakstøtte i ballistiske tester, Roma Plastilina. Leiren må testes i en ball drop test både før og etter det er brukt i testene på beskyttelsesutstyr. Siden det på Forsvarets forskningsinstitutt benyttes leire i mange ballistiske tester, er en bedre forståelse av denne leiren ytterst relevant. Dessverre er litteraturen mangelfull på dette området.

For å studere den ballistiske leiren benyttet på Forsvarets forskningsinstitutt er et par eksperimentelle ball drop tester blitt utført. Anslaget av stålkulen mot leiren ble filmet med høyhastighetskamera for å tillate dynamikken i penetrasjonen å bli observert. Disse eksperimentelle resultatene ble benyttet som referansepunkter for en rekke numeriske simuleringer. Elementmetoden i IMPETUS Afea programvaren ble brukt til å undersøke om det var mulig å simulere ball drop testene på pålitelig vis. Simuleringene ble først utført med en enkel modell for leire, hvor innflytelsen av den enkelte parametere ble studert. På denne måte kunne relevante parametere og tilføyelser til materialmodeller finnes.

Simuleringene viste at den initielle enkle modellen med lineær tøyningskurve ikke var tilstrekkelig god til å gjengi penetrasjonsdynamikken. I simuleringene viste stålkulen og leiren en for kraftig oscillasjon etter anslag. Andre og mer komplekse tøyningskurver ble testet, men bare med mindre forbedringer til følge. For å minske oscillasjonene i leiren etter anslag ble et dempningsledd innført i materialmodellen. Dette medførte mindre svingninger, men eksperimentene ble ennå ikke gjengitt på akseptabelt vis. Til slutt ble en viskoplastisk modell med innebygget demping testet. Med de rette materialparametere gjengav denne modellen de eksperimentelle resultatene på tilfredsstillende vis.

Med de rette parametrene viste simuleringene med den viskoplastiske modellen akseptable resultater innen de grenser for tøyningsrate, temperatur og plastisitet som ble observert i eksperimentene. Modellen er tilfredsstillende til å bli brukt i mer komplekse simuleringer med anslag av et hardkjerneprosjektil mot harde keramikkplater, ettersom usikkerhetene i materialmodellene for keramikk og hardkjernen til prosjektilet er ganske store. Men ytterligere arbeid på modellen for leire er nødvendig, dersom modellen må benyttes i simuleringer hvor leiren har større innflytelse på dynamikken. Modellen er likevel tilstrekkelig god for de simuleringene som planlægges.

Contents

1 Introduction

Harder, Better, Faster, Stronger. These are but some of the words describing the requirements for future equipment for the Norwegian Armed Forces, be it vehicles, weapons or clothing. The same is true for materials used for protection purposes. We want to increase the mobility of soldiers, without lowering their other capabilities in the field. A lower level of protection is a lower level of capability. Keeping the protection level high, while in the meantime lowering the burden from equipment for protection, requires improvements of the materials used. This is the aim of Forsvarets forskningsinstitutt (FFI) project 1301. The aim is to build sufficient knowledge to be able to contribute to the academic world and at the same time suggest ideas for improvements for Norwegian defence industry.

The main focus is on the ceramics used for protection for both personnel and vehicles against hard core threats, and on the composites and fibres used in conjunction with ceramic tiles. The approach is through both experiments and simulations. The ballistic tests have been performed on ceramic tiles with and without composites and fibres, but all of the tests have been performed with a backing of the oily ballistic clay. This has been done in order to keep the ceramic tiles in place and partly in order to mimic the human body.

From a modelling point of view this naturally means, that the clay also has to be included in the simulations. Despite the importance of being able to model the clay correctly, it is hard to find publications on this matter. In 2011 a PhD-thesis by C. I. Medina was published[1]. In the thesis Medina presents experimental results from torsion tests and compare these to model values, but no ball drop tests are discussed. In 2013, Medina and a group of scientists at Lehigh University published two reports for the Army Research Laboratory (ARL)[2, 3]. In these reports both experimental and simulation results for the ball drop tests are presented. From these reports a starting point for the parameters used in modelling the clay can be found. The modelling results are interesting, however, they are for some unknown reason consistently presented with a time-scale that appears to be a factor of 10 wrong[1]. On the same note it should be mentioned that the experimental results are presented without units, so only the shape of the penetration curve as function of time can be used further. However, a few main points from the ARL-reports can be used in the simulation study in this work. First, the most important parameters for clay in the simulations are the elastic modulus and the yield stress curve. Second, the presented parameters (from experiments) for the elastic modulus and the stress-strain curves of clay are useful as guidelines for the parameters used in the simulations.

Due to the uncertainty about the experimental ball drop test results in the ARL-reports, it

---

[1]This statement is based on simple comparisons of Newtons laws and the results presented in [3]. Moreover, a brief look at Figures 33 and 34 in the same report proves as excellent examples of that something is not right. The highest acceleration (deceleration) of the steel ball upon impact with the lay is given as 265 in/s^2, which in SI-units is 6.73 m/s^2 - which is even lower than gravity. This will not force the ball to stop within a few cm.

was decided to perform a few ball drop tests in the ballistic lab at FFI, to have experimental data as comparison to the simulation results. The main goal with the simulations is to test whether the simple initial material model used in the simulations at FFI adequately describes the clay. The model is expanded and parameters varied step by step until a material model with material parameters describe the clay performance in a satisfactory manner. When this is achieved, we are one step closer to being able to simulate larger and more complex systems involving clay, ceramic and projectile.

2 Ball drop experiments

The test-standards from the American National Institute of Justice (NIJ) for ballistic protection for personnel require that vests and plates are tested with Roma Plastilina No. 1 (an oil-based modelling clay) as backing material. The clay is used to model the human body, and the deepest deformation allowed in the clay after an impact is 44 mm. Before and after the experimental test, the clay is subjected to a ball drop test in order to ensure that the clay meets the requirements set up by the NIJ 0101.06 standard[4]. The clay is tested by dropping a steel ball with a diameter of 63.5 mm and a mass of 1043 g from a height of 2 m onto the clay and measuring the depth of the crater under the ball. The test requires the arithmetic mean of 5 drops to be 19 ± 2 mm.

Besides the above mentioned requirements, there are requirements such as a fixed temperature of the clay, humidity in the room and the size of frame containing the clay. These requirements have been omitted for the experiments presented in this work. The NIJ Standard should be followed strictly when companies producing body armour test their products. However, in the case of studying the clay used at FFI, it makes more sense to study the clay as it is actually used in all other tests at FFI. For this reason the ballistic clay used for the experiments presented below was previously used for other experiments and the metal frame containing the clay did not have the correct size according to the NIJ Standard. However, the size, material type and mass of the ball was well within the requirements.

2.1 Experimental setup

(a) The experimental set-up after a ball drop test. The steel ball is seen in the middle of the clay.

(b) The crater depth is measured with a calliper with the frame as reference after an ball drop test.

Figure 2.1   Images showing the full experimental setup and the measurement of the crater depth.

The aluminium box, size $0.71 \times 0.71 \times 0.115$ m, filled with clay was positioned a few cm above ground on a few pieces of wood in order to avoid any effect of the concrete floor. This

position allowed the steel ball to be dropped from a height of 2 m as required. The Phantom high speed camera was positioned at the same height as the top of the clay so the impact could be filmed from a horizontal angle. The clay box was lit up by three high intensity lamps. The experimental setup is shown in Figure 2.1a. The camera was set to a frame rate of 6000 fps, which with an impact speed of roughly 6.25 m/s corresponds to a movement of the ball of roughly 1 mm per frame. To be able to hit the region covered by the high speed camera, the ball was dropped through a plastic pipe. This will naturally have small effect on the velocity of the ball, since the air resistance will be slightly higher inside the pipe. This effect is, however, expected to be smaller than the effect from the uncertainty in the drop height. Besides, the velocity of the steel ball at impact can be found from the high speed videos. The diameter of the steel ball was measured to 63.5 mm, and the mass was found to be 1048.0 ± 0.1 g. Before each of the two experiments, the clay was levelled with a wooden hammer. After the experiments, the depth of the crater was measured with a calliper.

No tape measure was used in the experiments. Since the diameter of the steel ball is well known, this can be used to find the size of a pixel in the videos. The velocity of the steel ball in the two tests was found from the high speed videos by measuring the position of the top of the steel ball in the frames just before impact with the clay and then converting these to a velocity. The depth of the penetration could not be measured as such in the experiments. However, by assuming that the steel ball does not deform or bounce away from the clay during the impact, the penetration depth can be estimated by tracking the position of the top of the steel ball. This tracking was done in the freeware software ImageJ[2] using the MTrakcJ plugin[3]. With this software the position (in pixels) of the top of the steel ball can be recorded for each frame. From this the position can easily be found in the analysis.

The crater depth was measured manually with the calliper as shown in Figure 2.1b. Upon impact the clay is pushed to the side and an elevated crater edge is seen around the impact position. For this reason the penetration depth was to be measured with the aluminium frame as a reference.

2.2 Experimental results

The results from the experimental ball drop tests are shown in Figure 2.2. The figure shows the penetration depth of the ball into the clay as a function of time from initial contact with the clay. The velocity of the ball before impact was found to be 6.3 m/s and 6.2 m/s for tests 1 and 2, respectively. The theoretical impact velocity is 6.27 m/s (no air resistance and $g = 9.82$ m/s^2), so the use of the plastic pipe in the experiments did not appear to have a significant effect on the impact velocity.

In the second drop the penetration depth was measured to be 22 mm (and 24 mm from the

---

[2]`http://imagej.nih.gov/ij/`
[3]`http://www.imagescience.org/meijering/software/mtrackj/`

top of the crater edge). In the first impact the reference measurement was unfortunately forgotten, so only the depth form the craters edge was measured. This was found to be 23 mm.
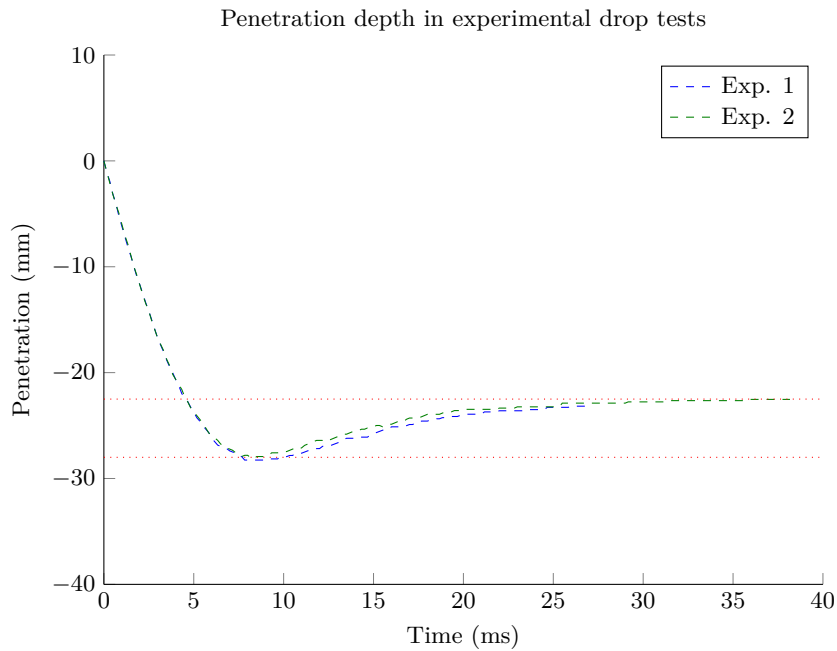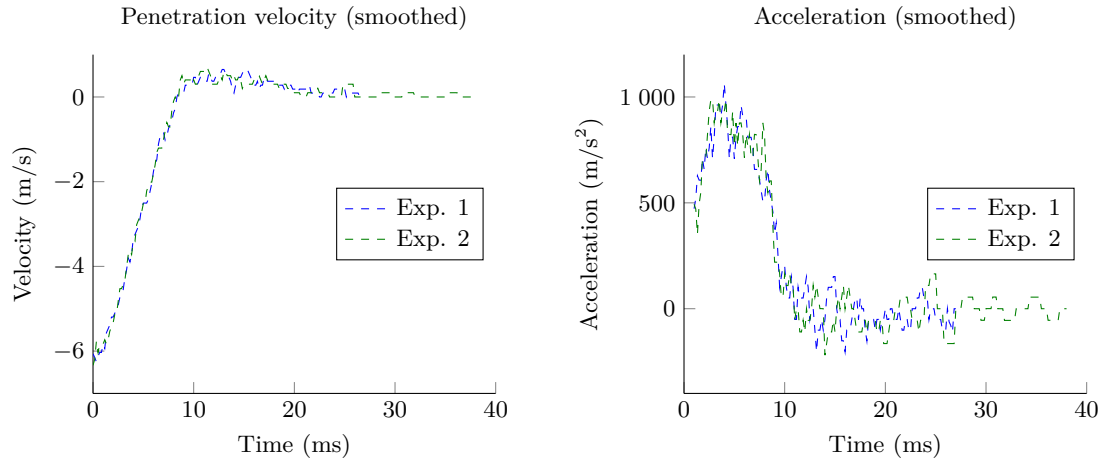

Figure 2.2   *The penetration depth as a function of time for the steel ball in the experimental drop tests. For both tests it is clear, that the ball has penetrated roughly 28 mm into the clay after ~ 8 ms, after which the clay behaves partly elastic and recovers back to a final penetration depth of $22-23$ mm. The two red dotted lines represent penetration depths of 22.5 mm and 28 mm.*

From the experimental result in Figure 2.2, it is hard to tell what the velocity and the acceleration of the steel ball is during the impact with the clay. To get an estimate of the velocity as a function of time, the penetration data has been differentiated. Next the acceleration can be found by performing the same routine on the velocity data. Due to the limited precision of the depth measurements and the relatively low number of data points, this unfortunately results in large scattering of the data points for the velocity and even worse for the acceleration. For this reason both the velocity and the acceleration data has been smoothed using a moving average smoothing function with a span of 7 and 11, respectively. The fact that the data has been smoothed does, however, not mean that the results are not trustworthy. The general trend is not affected by the smoothing, and it is this trend that is interesting.

The results for the velocity and acceleration are shown in Figures 2.3a and 2.3b. The velocity curve shows that the ball gains a positive velocity after 8 ms, which means that it moves upwards. This is a result of a partial elastic behaviour of the clay. It takes roughly 3 ms for the acceleration to reach the maximum. This is not surprising as the contact

(a) The figure shows the velocity of the steel ball in the two drop tests. The velocity is found by differentiating the penetration depth as function of time. The data was smoothed by a moving average function with a span of 7 to avoid extensive scattering of the points.

(b) The figure shows the acceleration of the steel ball (found by differentiating the velocity) in the two drop tests. Smoothing based on a moving average with a span of 11 was applied to the data. The first 5 data points was removed due to extensive scattering.

Figure 2.3   Figures showing the velocity and the acceleration of the steel ball in the two experimental tests. The results are the first and second derivative of the ball position seen in Figure 2.2.

surface between clay and the ball is small in the beginning. After the maximum acceleration of close to 1000 m/s^2 has been reached, the acceleration falls to 600 m/s^2 over the next few milliseconds. At $t = 8$ ms the acceleration is close to zero, and the direction of the velocity is reversed. The found values for the acceleration is in stark contrast to the numbers presented in [3]. The maximum acceleration in their simulation is 265 in/s^2, which corresponds to 6.73 m/s^2. With this deceleration, the ball requires 0.93 s to slow down to zero velocity. As before-mentioned, this could be due to the possibility of the time-scale in their simulation being off by a factor of 10. If the time-scale is divided by this factor 10, the maximum deceleration in their simulation becomes 673 m/s^2, which is more realistic.

3 Simulations

The simulations in the work has been performed with the IMPETUS Afea software package. With this software it is possible to perform simulations using the Finite Element Method (FEM). In the FEM, the simulations are performed by dividing the problem at hand into smaller sub-units of cells, that combined mimic the real problem. A set of sub-units or cells is called a mesh or a grid. The advantage of this approach is that for a given, and often small, time-step, the numerical simulation can essentially be performed individually for each of the sub-units. After each time-step, the results of the calculations for each sub-unit are collected and the resulting, new forces and pressures are used as inputs for each sub-unit in the calculations for the next time-step.

There are several methods of how to model these sub-units, Lagrange, Euler and Smooth Particle. The IMPETUS software package used for this work is built upon the Lagrange approach. In this method, the material that is initially within a given sub-unit stays within that sub-unit throughout the simulation. Any deformations are made on the sub-units, which means that the initial grid is allowed to be deformed during the course of the simulation.

The response of a given sub-unit is based on the material model and properties assigned to the larger unit that the sub-unit is a part of. In the IMPETUS software package the material models can be chosen from a set of built models. In order to get reliable results from FEM simulations, the initial grid, the material models and the material parameters have to be chosen with care.

3.1 Material models used for the ballistic clay

In literature, clay such as Roma Plastilina has been modelled by the Drucker-Prager model. The Drucker-Prager model is a pressure-dependent model that is usually used for modelling soil and other materials that undergo substantial plastic deformation. Unfortunately, this model is not included in the IMPETUS Afea software. Instead, the clay has been tried modelled as a metal using the *MAT_METAL keyword and with the *MAT_VISCO_PLASTIC keyword.

The *MAT_METAL is essentially the modified Johnson-Cook (MJC) model [5]. This model is discussed in more detail in Section Appendix A. One of the main reasons for using the *MAT_METAL model to model the clay is that it allows for a user defined yield stress response. This means, that the the clay is not modelled by the usual MJC yield stress vs. strain function, but instead from a user-defined curve. Various shapes and values were tested for the hardening response. Initially, simple linear yield stress responses were tried. Next, yield stress curves closely resembling experimental results from [2] were used. One of the conclusions from the work done at ARL, was that the penetration depth primarily depended on the yield stress curve and the elastic modulus. For this reason, the Poisson

ratio of the clay was kept constant at a value of $\nu = 0.49$ in this work.

The IMPETUS Afea software package has a built in model for visco-plastic materials, called by keyword *MAT_VISCO_PLASTIC. The model is explained in more detail in Section Appendix A. The *MAT_VISCO_PLASTIC model is somewhat different than the *MAT_METAL. But for the parameters used in these simulations, the most important difference is the way the yield stress curve is defined and the possibility to make the material viscous. The yield stress curve can be made dependent on pressure, which means that it is possible to have a yield stress that increases with confining pressure. The viscosity in the model results in a damping effect in the material.

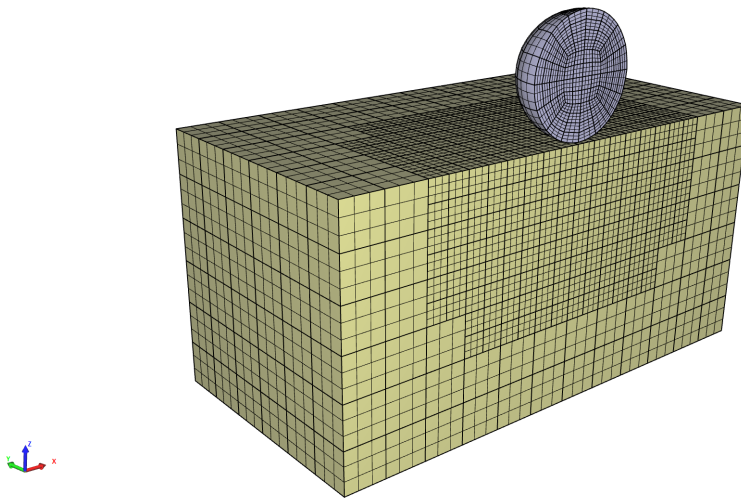### 3.2 Construction of the simulation model setup

Figure 3.1   The figure shows an angled view of the mesh used in the simulations of the ball drop test. In the simulations, the XZ-plane is used as a symmetry-plane, which reduces the number of elements and nodes and gives a lower simulation time. In the central region, where the deformation of the clay is expected to be highest, the mesh is refined by a factor of 2.

The mesh and set-up used as starting point for the simulations is shown in Figure 3.1. A symmetry plane is added in the XZ-plane in the simulations in order to lower the computation time. This means that only half of the sphere and clay box is modelled. The clay was modelled with a thickness of 0.14 m, and the sides of the box is 0.28×0.14 m (reduced from 0.28×0.28 m by symmetry). The width is smaller than the clay box used in the experiments, but in order to keep the computational cost down, the size was lowered. This is however, not expected to have drastic effects on the results.

The clay is divided into elements with a side length of 2.33 mm, and the elements within a sphere with a radius of 0.105 mm of the impact point are refined by a factor of 2. The length of an element in the refined region of the clay is then 1.17 mm, which is close to

the 1.27 mm used in the second ARL-report[3]. All the elements in the clay are changed from linear to cubic elements by the *CHANGE_P_ORDER keyword, in order to improve their behaviour in plasticity. The sides and the bottom of the clay is constrained from movements in all directions. The steel ball is modelled as an elastic material with the properties found in Table 3.1. The steel ball, diameter 63.5 mm, is positioned a distance of 1 mm above the clay at simulations start with an initial velocity of 6.276 m/s. Gravity is set to $g = 9.82$ m/s^2.

In the following sections, results from some of the simulations are presented. The penetration depth of the steel ball is shown as a function of time. The depth is taken as the z-position of the node in the clay directly under the center of the steel ball. This node, and not the bottom node of the steel ball, was chosen, because the steel ball bounced off the clay in many of the simulations, due to a lack of damping in the clay models.

3.3 Initial model for clay

Initially, the clay model was set up by Jeffrey Simons from SRI International. Since the work presented in this report is only a part of a larger study on impact of hard core projectiles on ceramic tiles backed by clay, the clay model was not the first parameter to be studied in detail. So for many of the simulations in the full study, this initial clay model was used since it gave results in the right ballpark. However, as a result of the outcome of the work presented here, the clay model used in the projectile impact simulations has been updated.

Table 3.1   Table showing some of the material parameters used for the steel ball and the clay in the drop test simulations.

Property	Steel	Clay
Elastic modulus [MPa]	210000	1-20
Poisson's ratio	0.29	0.49
Density $\left[\text{kg/m}^3\right]$	7780	1570

For the initial clay model the *MAT_METAL material model was used with parameters shown in Table 3.1. The yield stress curve for the model is used with the simplification as described in Appendix A. At zero strain, $\epsilon = 0$, the yield stress is 65 kPa, and this increases linearly to 155 kPa at $\epsilon = 1$. The resulting curve is the blue curve in Figure 3.4. For higher strains, the yield stress is kept at 155 kPa.

The result of a simulated ball drop test with the initial clay material parameters is shown in Figure 3.2 together with the experimental results. In the simulation the steel ball penetrates more than 37 mm into the clay on impact. Hereafter, the clay partly recovers elastically and oscillates around 30 mm. The oscillation is due to the lack of viscous damping in the clay model. From the comparison to the experimental results it appears that the clay is modelled as too soft. In order to find out if this is due to the elastic modulus or the yield

stress, the effect of these parameters were studied separately.

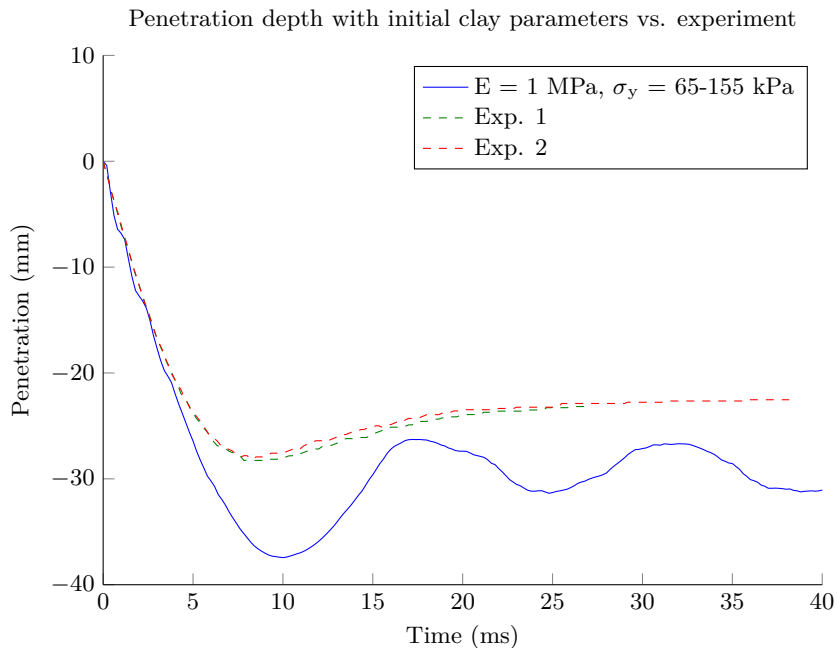Penetration depth with initial clay parameters vs. experiment

*Figure 3.2   The figure shows the penetration depth of the steel ball into the clay using the
initial material parameters for clay. It is clear that the penetration into the
clay is too deep when compared to the experimental results. The velocities for
experiments 1 and 2 were 6.3 m/s and 6.2 m/s, respectively.*

3.4   Effect of the elastic modulus

As seen in the previous section, the initial material parameter used with the MJC-model
resulted in too deep penetration into the clay, as seen in Figure 3.2. Furthermore, the
behaviour of the clay was too elastic, visible by the oscillation in the depth after impact.

As a first method to lower the impact depth into the clay, the elastic modulus of the clay
was increased. The initial elastic modulus was 1 MPa. In the two ARL studies[2, 3] elastic
moduli of 4.136 MPa and 6.58 MPa are used to model the clay. Simulations have been
performed with these two values as well as elastic moduli of 2 MPa and 20 MPa.

The results of the simulations are shown in Figure 3.3. The results of the simulations
clearly show, that as the elastic modulus increases the initial penetration depth decreases.
The final penetration depth, however, does not become much smaller (only 1-2 mm) with
increasing elastic modulus. This is due to the fact that the yield stress curve is the same in
all simulations. The yield stress curve explains at which stresses the clay behaves plastically
instead of elastically. When the stress in the clay reaches a point on the yield stress curve
the behaviour becomes plastic. So even though the elastic modulus is different in these
simulations, the plastic behaviour sets in at the same stresses. So the main effect of the
elastic modulus is to change the initial penetration depth before the clay bounces back
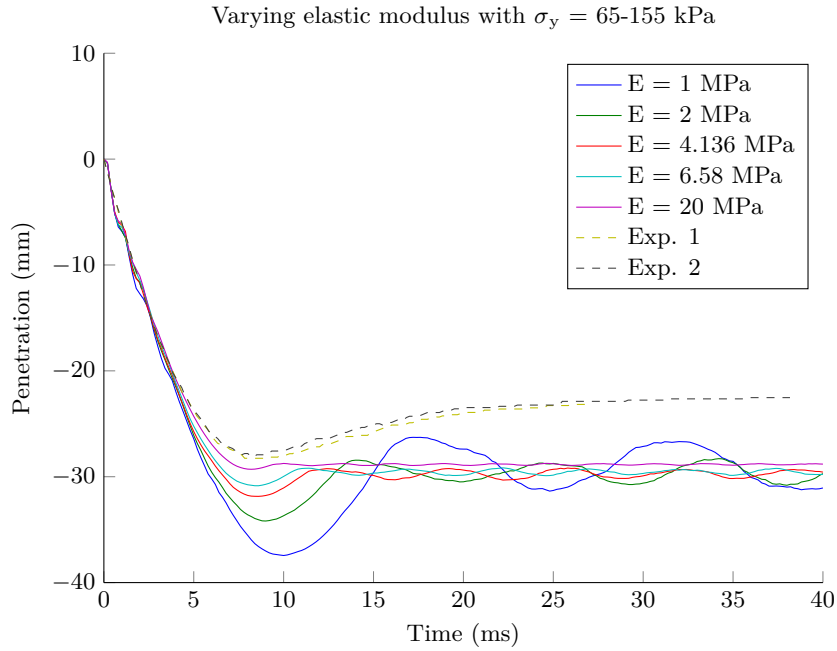
*Figure 3.3   This figure displays the penetration depth of the steel ball into clay modelled
with various elastic moduli. The yield stress curve is kept constant for the five
elastic moduli.*

upwards.

From the results it is clear that the highest elastic modulus of 20 MPa is too high (with
the current yield stress curve), since the elastic effect of the clay has practically vanished.
None of the elastic moduli in the range of 1-6.58 MPa, can be discarded without a study
on the effect of the yield stress curve.

3.5   Linear yield stress functions

The yield stress curve used in the initial simulation, the blue curve in Figure 3.4, has a
linear dependence of strain. At a strain of 0, the yield stress is 65 kPa. The yield stress
increases linearly up to a strain of 1 where it reaches a maximum and stays at 155 kPa
even for higher strain levels. To study the effect of the yield stress on the penetration into
the ballistic clay, simulations were performed with four other linear yield stress curves. The
yield stress curves are shown together in Figure 3.4. In order to try to achieve a smaller
penetration into the clay, the yield stresses have been increased when compared to the
initial parameters. The simulations have been performed with elastic moduli of 1 MPa and
6.58 MPa, since the results based on the results shown in the previous section.

The results of the simulations are shown in Figures 3.5a and 3.5b for 1 MPa and 6.58 MPa,
respectively. It is clear from the penetration curves, that higher yield stress values results in
less penetration into the clay. It is also evident that higher yield stresses results in a more
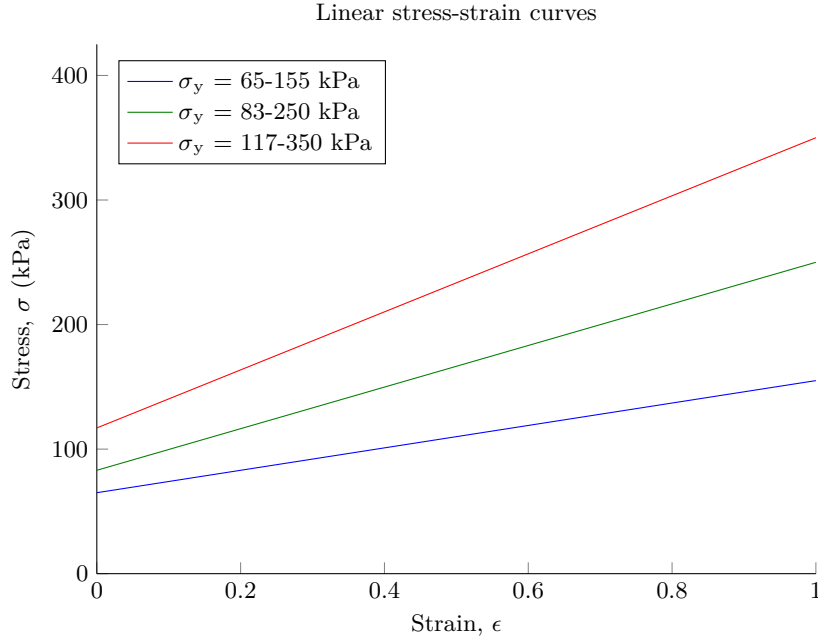
Figure 3.4 The yield stress curves used to study the effect on the penetration depth into clay. The blue curve (σ_y = 65-155 kPa) is the initially used parameters.

elastic behaviour of the clay for both values of the elastic modulus. Unfortunately, none of the simulated penetration depth curves match the experimental results. The oscillating behaviour can be dealt with (to some extent) by increasing the elastic modulus. However, this also lowers the initial penetration depth too much. From the results presented in Figures 3.5a and 3.5b it is seen that higher values for the yield stress results in lower penetration depth. It appears as if the approach with linear yield functions is somewhat too simple to reproduce the experimental results.

3.6 Non-linear yield stress functions

In order to get a more realistic behaviour of the clay in the simulations, experimental results for yield stress curves of the ballistic clay have been found in the report Pamukcu and co-workers[2]. They performed uni-axial compression tests on new clay, remolded clay and heated, remolded (41° C) clay. From these experiments they extracted a measure for the stress-strain curves (yield stress curves) for the clay. The results for the remolded clay (which is probably most likely to match the clay used in our drop tests) are shown in Figure 3.6a, while the heated and remolded clay response is shown in Figure 3.6b. As can be seen from the curves for the remolded clay, the stress is dependent on the velocity (strain rate) with which the tests are performed. For a higher strain rate the yield stress curve has higher values for a given strain. However, not even the highest of the test velocities, 7 mm/min, is close to being comparable to the velocity in the ball drop tests, 6.26 m/s = 375600 mm/min. Despite this difference in velocity (strain rate) in the experiments, it is

Varying linear yield stress with E = 1 MPa

Varying linear yield stress with E = 6.58 MPa
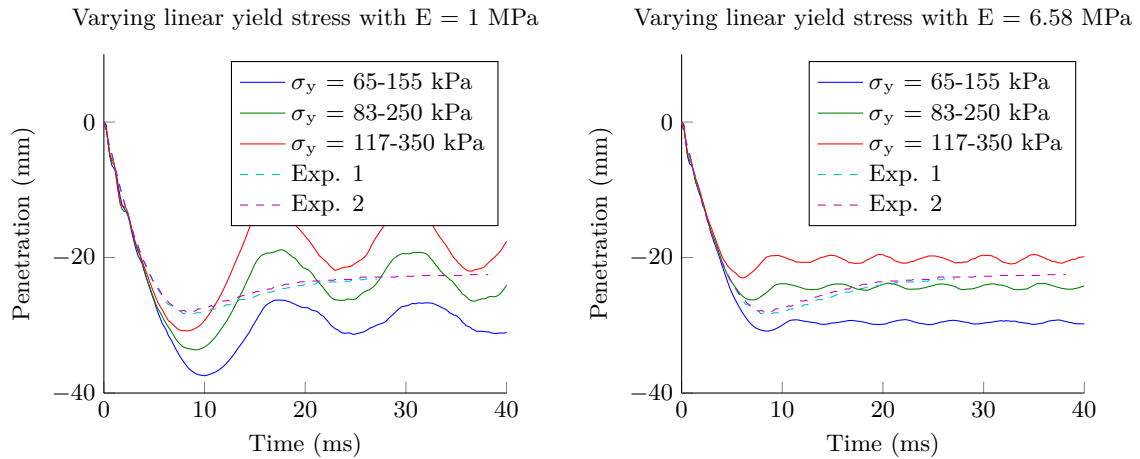
(a) Simulated drop tests with E = 1 MPa.

(b) Simulated drop tests with E = 6.58 MPa.

Figure 3.5   The results of the simulated drop tests with varying yield stress curves. The blue curves are the result with the initially used yield stress parameters (σ_y = 65-155 kPa) and the dashed lines are the experimental results.

interesting to test these experimental yield stress curves in the simulations. The general trend seen in Figure 3.6a and 3.6b is that the increase in yield stress is most significant for lower strain and that the yield stress levels off and becomes strain independent above strains of ~ 0.2.

Figure 3.7 shows the yield stress curves used in the simulations. The green curve, C2, is very similar to the experimental curve at 7 mm/min. For the blue curve, C1, the yield stress is made somewhat higher than the experimental curves shown here. This curve is made to match the response for new clay. The fact that the blue curve is lifted a little toward higher stresses for all strains could make it be closer to an actual response for the remolded clay at higher strain rates.
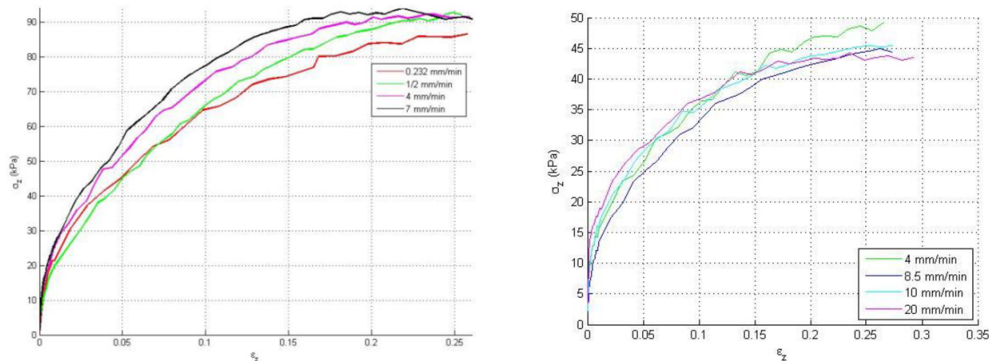
(a) Yield stress curve for remolded clay (reprinted from [2]).

(b) Yield stress curve for remolded and heated clay (reprinted from [2]).

Figure 3.6   The figures show the result from an uni-axial compression tests performed by Pamukcu and co-workers[2].
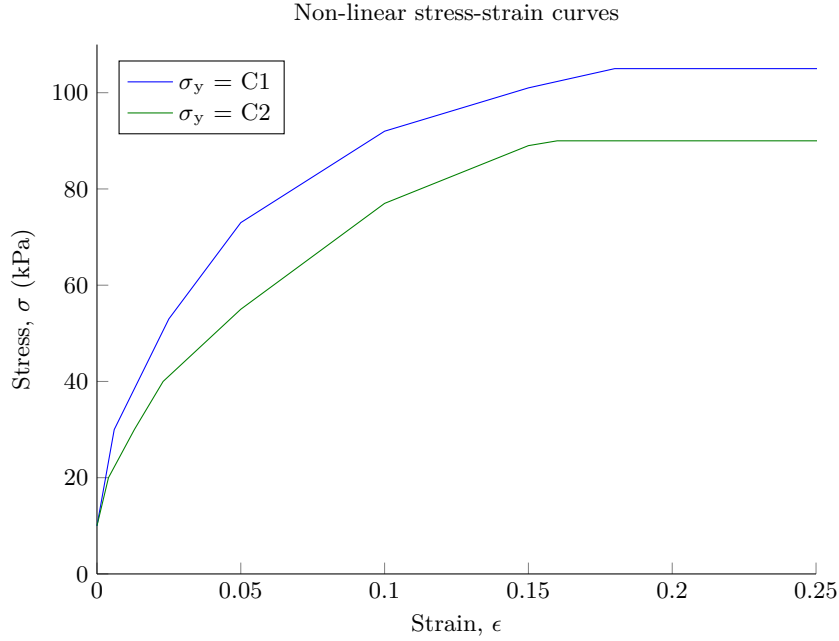
Figure 3.7 *The two non-linear yield stress curves tested in the simulations. The green curve, C2, is very similar to the experimental curve for remolded clay at the highest compression rate (7 mm/min), while the blue curve, C1, is for new clay, but might be closer to the clay response at higher compression rates.*

Figure 3.8 shows the the results of the simulated drop tests with non-linear yield stress and an elastic modulus of $E = 1$ MPa. The results with the two non-linear yield stress curves are compared to the experimental results and the simulation results with the initial linear yield stress curve. Although the yield stresses for the non-linear curves are lower (10-105 kPa and 10-90 kPa for C1 and C2) than for the initial yield stress curve (65-155 kPa), the response of the clay for these three are not that different. As expected, the penetration into the clay modelled with yield stress C1 is less than with the lower yield stress of C2. The clay modelled with C1 allows less penetration than the initial input, while with C2, the response of the clay is somewhat softer than with the initial input. The reason that these two lower yield stresses can lead to a similar response as the initial parameters is that the yield stress increases to its maximum value at a strain of 0.15 for C1 and C2, whereas the maximum value for the initial input is not reached until a strain of 1.0. Since C1 and C2 match the experimental stress-strain curve obtained form a uni-axial compression test, these are interesting to study further. None of the simulations presented so far have been able to reproduce the non-oscillating behaviour of the clay seen in the experiments. In order to be able to minimize this elastic response of the clay, a damping coefficient can be added to the clay parameters.
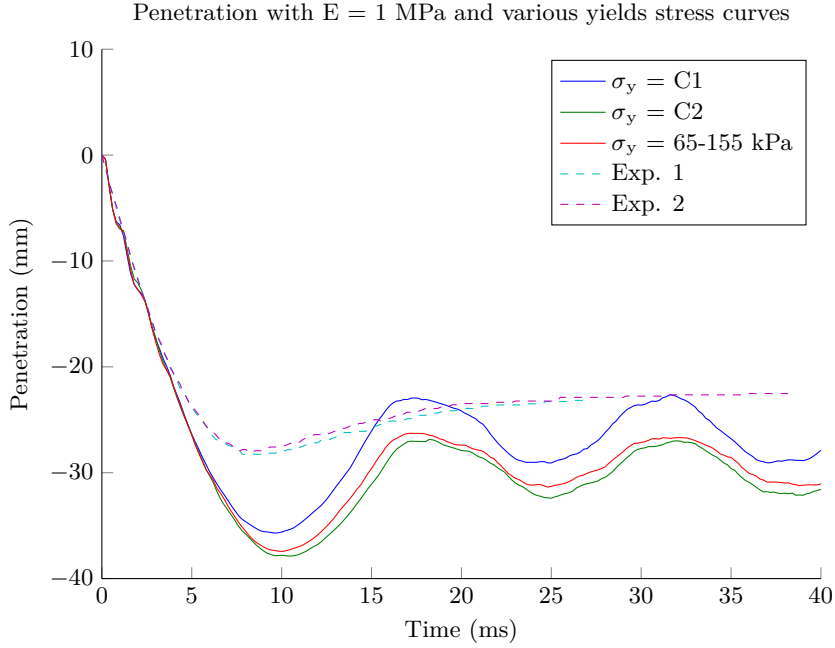
Figure 3.8   Penetration into the clay modelled by the non-linear yield stress curves, C1 (blue) and C2 (green), and the initial input parameters (red).

3.7   Effect of damping

Damping in the clay was added by the *LOAD_DAMPING keyword. This keyword adds a damping term to the material given by

$$\sigma_\mu(t) = \frac{\mu}{c_{dec}} \int_0^t \dot{\epsilon}(\tau) \, \mathrm{e}^{(-\tau/c_{dec})} d\tau, \tag{3.1}$$

where $\dot{\epsilon}$ is the actual strain rate, μ is the damping coefficient and c_{dec} is the strain rate decay constant. As c_{dec} approaches 0, $\sigma_\mu(t)$ approaches $\sigma_\mu(t) = \frac{\mu}{c_{dec}}\dot{\epsilon}(t)$. In the simulations the decay constant, c_{dec}, has been kept low (0.1 ms), rather than increasing μ.

The resemblance of Equation 3.1 to the usual definition of viscosity is in the strain rate dependence. Usually, the force from viscosity is defined as being proportional to the velocity of the part moving in a viscous medium. In Equation 3.1 the force is proportional to the strain rate, which is essentially proportional to the velocity.

The results of simulations with yield stress curve 1 from Figure 3.7 and damping terms, $\mu = 0.2\ kPa$ and $c_{dec} = 0.1$ ms, is shown in Figure 3.9a for E varying from 1-6.58 MPa. It is clear that the applied damping is not adequate to reproduce the experimental results, but it is clear that the elastic modulus should not be in the higher end of the range as this will result in too small an elastic effect with a larger damping term.

In Figure 3.9b the results of simulations with an elastic modulus of $E = 2$ MPa, $c_{dec} = 0.1$ ms

Penetration with $\sigma_y = $ C1 and $\mu = 0.2$ kPa

Penetration with $\sigma_y = $ C1 and E $= 2$ MPa
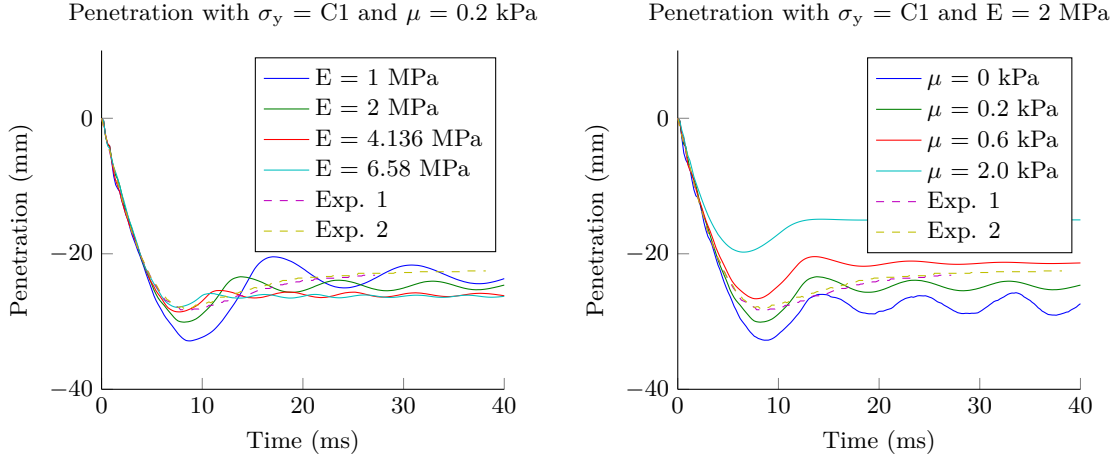
(a) *The penetration depth for clay modelled with damping, decay constant $c_{dec} = 0.1$ ms. The oscillations becomes lower at longer times, but the damping term may be too small to properly match the experimental results.*

(b) *Penetration in the clay with $c_{dec} = 0.1$ ms and different values for the damping constant μ. A higher value for μ does result in less oscillations, but the penetration depth becomes too small for increasing μ.*

Figure 3.9   Figures of the penetration with varying values for E and the damping constant μ.

and μ ranging from 0.2-2 kPa. The penetration into the clay shows markedly less oscillating behaviour for larger values of the damping coefficient. However, for $\mu = 2$ kPa the clay is too stiff and the penetration into the clay becomes too small. With $\mu = 0.6$ kPa response of the clay is closer to the experiments, but a slower rebound and a little deeper penetration initially would make for a better match. This could partly be realized by lowering the elastic modulus somewhat. Unfortunately, this also results in larger oscillations. Instead of trying to adjust the *MAT_METAL material model further, the experience gained with this model was used to simulate the clay with the *MAT_VISCO_PLASTIC material model.

3.8   Visco-plastic material model

The *MAT_VISCO_PLASTIC material model is explained in detail in Appendix A. This material model includes a non-linear viscous term (which is essentially the same as including the keyword *LOAD_DAMPING), a non-linear elastic term and a linear elastic term. The yield stress for this material keyword is given by Equation A.9. This is simplified, by leaving temperature dependences and assuming no pressure dependence[4]. The yield stress is thus determined by the following equation

$$\sigma_y = \sigma_0 + Q\left(1 - \mathrm{e}^{-C\epsilon^p_{eff}}\right). \tag{3.2}$$

---

[4]The yield stress of the clay is expected to have some dependence of pressure, however, results by [2] show that for remolded clay this effect is very small. A pressure dependence was included in some simulations, but the results for the values tested were not significantly different than without.

Simulations have been performed with the yield stress function in Equation 3.2 adjusted to match the experimental curves from [2]. The values for the parameters σ_0, Q and C are shown in Table 3.2. The yields stress curves are displayed in Figure 3.10 The values for VP2 makes the yield stress curve resemble 'curve 1' used previously. Thus, VP2 would match new (unmolded) clay or remolded clay at a high strain rate, see Figure 3.6a. The yield stress curve for VP3 is adjusted to mimick the properties of remolded and heated clay, as seen in Figure 3.6b. The yield stress curves of VP4 and VP5 are both in between VP2 and VP3.

Table 3.2   Table showing the material parameters used for the steel ball in the drop test simulations.

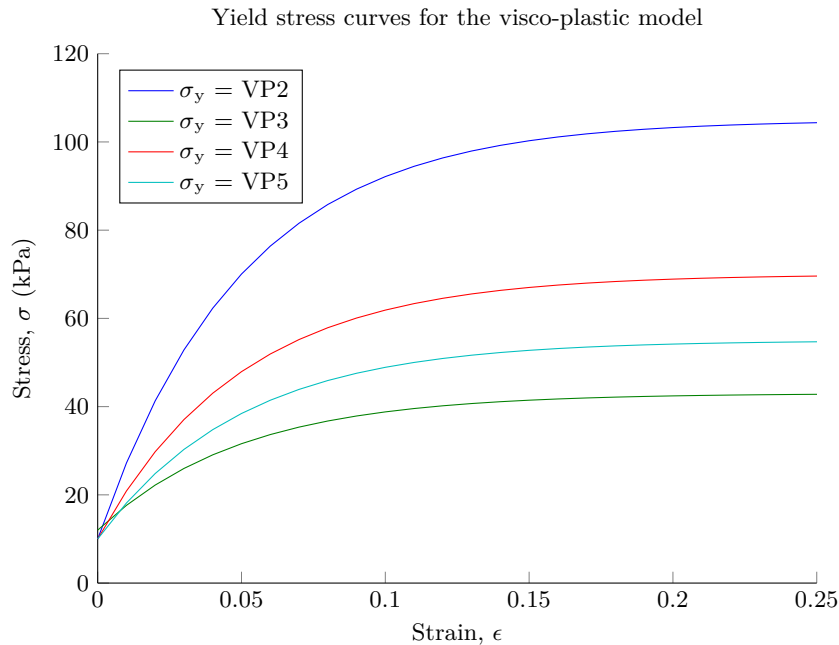|	σ_0 [kPa]	Q [kPa]	C
VP2	10	95	20
VP3	12	31	20
VP4	10	60	20
VP5	10	45	20

Figure 3.10   The yield stress curves used in the visco-plastic material model for clay. VP2 (blue) is very close to new clay, while VP3 (green) resembles remolded and heated clay.

In Figure 3.11, results with clay modelled by the *MAT_VISCO_PLASTIC material model are shown. The elastic modulus was kept at $E = 1$ MPa, with $c_{dec} = 0.1$ ms and $\mu = 1$ kPa. It is clear that the visco-plastic material model is better at describing the behaviour of the clay under plasticity. The oscillating behaviour of the clay is much less pronounced. Interestingly, the results also show, for the chosen clay properties, that the VP2 (new clay)

parameters result in too low penetration, while VP3 (remolded, heated clay) parameters result in a deeper penetration into the clay. VP4, which is in between the two, gets the initial penetration just right. This is a reassuring result, since the clay used in our experiments was neither new, nor was it heated and remolded, but could be expected to have properties somewhere in between the two.
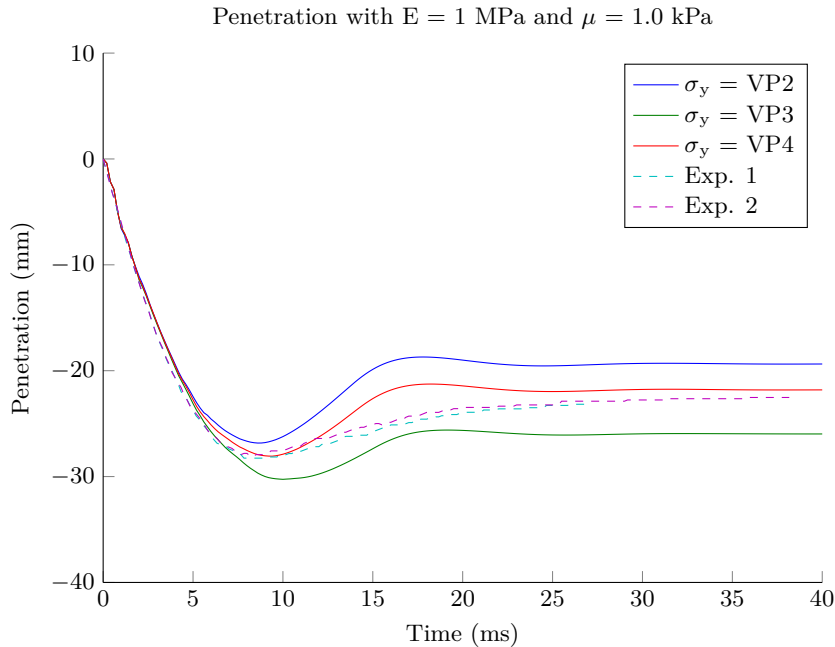

Figure 3.11   Simulation results for three different yield stress functions for the visco-plastic material model, with $E = 1$ MPa, $\mu = 1.0$ kPa and $c_{dec} = 0.1$ ms. The plasticity and damping terms for this model effectively minimizes the oscillations of the clay.

In order to test if the results discussed above (VP4 being better than VP2 and VP3) were due simply to the viscosity term, μ, both VP2 and VP3 were tested with variations in μ. For VP2, shown in Figure 3.12a, the drop test is closer to the experiment for a lower decay constant $\mu = 0.6$ kPa, but not better than what was found for VP4. The initial penetration is too deep, and some oscillatory behaviour as also seen at later times. For VP3, see Figure 3.12b , the result is quite good with a decay constant of $\mu = 1.3$ kPa. The deepest point in the penetration is perhaps reached a little late compared to the experiments.

The yield stress curve for VP3 is valid for a remolded and heated clay, which is not completely representative for the clay used in the experiments, so it was tested if VP5 would also be able to reproduce the experimental results. It was found that changing c_{dec} to 0 gave essentially the same result as with 0.1 ms, so $c_{dec} = 0$ was used for the simulation, with $\mu = 1.1$ kPa and $E = 1$ MPa. The outcome of the simulation is compared to the experimental results in Figure 3.13. As the plot shows, the simulation reproduces the experiments fairly well apart from the rebound from 15-20 ms. The depth of the penetration
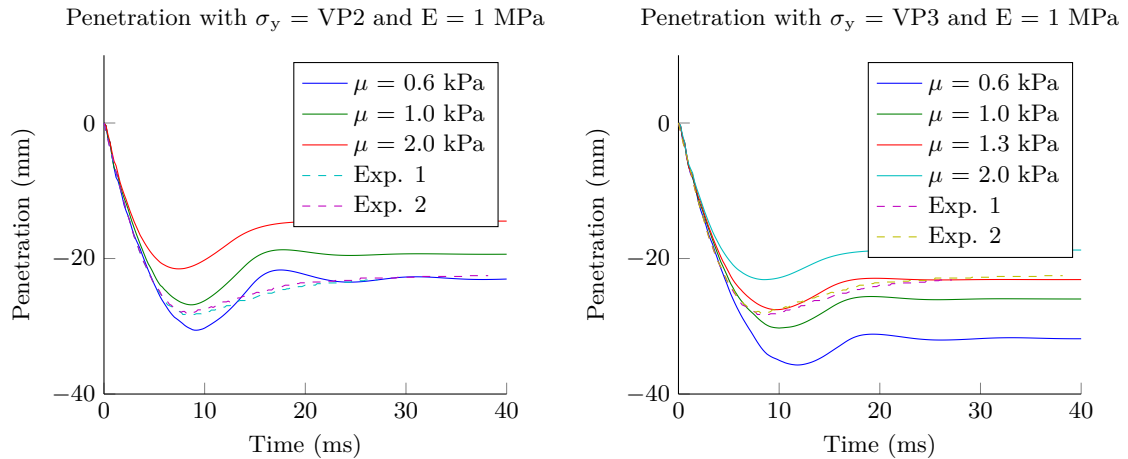
(a) Penetration curves for VP2 with three values for μ ($E = 1$ MPa and $c_{dec} = 0.1$ ms).

(b) Penetration for VP3 with four different values for μ ($E = 1$ MPa and $c_{dec} = 0.1$ ms).

Figure 3.12   Figures showing the results for clay with different values of the damping term μ. The effect of the yield stress parameters are visible by comparing the two figures.
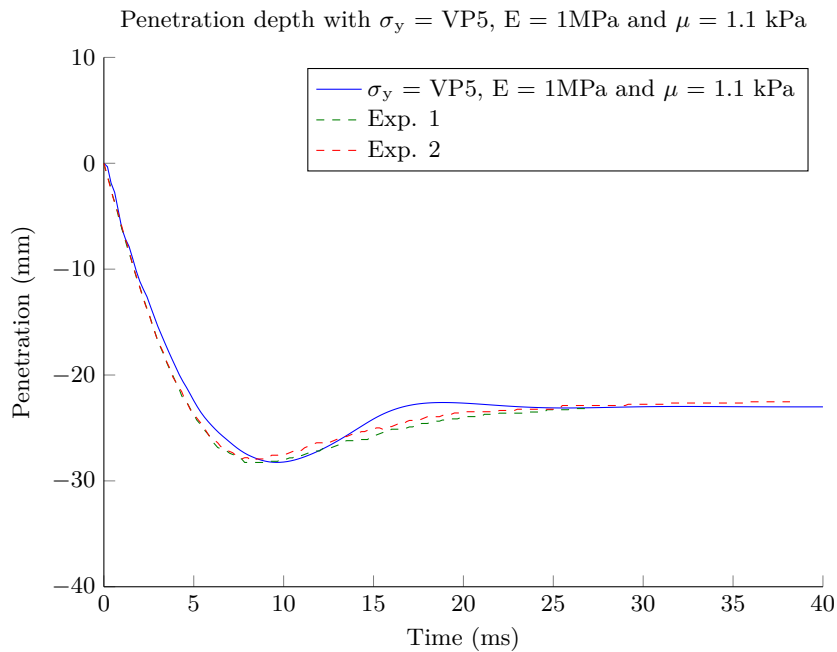

Figure 3.13   Simulation results for VP5 with a damping term of $\mu = 1.1$ kPa, $E = 1$ MPa and $c_{dec} = 0$ ms. The simulation is an acceptable match to the experiments.

matches perfectly and the final position of the steel ball is within 1 mm of the experiments. The results could be refined further by varying E, μ, c_{dec}, σ_0, Q and C, however, for the time being the model and the parameters shown in Figure 3.13 are more than adequate for use in the more complex impact simulations with ceramic and hard steel core projectiles.

4   Conclusion

The experimental ball drop tests performed at FFI showed a response of the clay that was both elastic and plastic. During impact the steel ball penetrated roughly 28 mm into the clay, but due to a partial elastic behaviour of the clay, the ball and clay rebounds a few mm up to the end position of 22-23 mm.

This experiment was modelled with IMPETUS Afea. As a first approach, the clay was modelled with the *MAT_METAL model (MJC), which was developed for metals. The initial hope was that a relatively simple model for the clay would be able to reproduce the experiments. However, as the results in Figures 3.5a and 3.5b show, the response of the clay with linear yield stress curves is not able to reproduce the results. The lack of a damping term in the model results in an oscillatory behaviour of the clay.

Although the simulations with the simplified MJC model did not give satisfactory results, they did show that the elastic modulus for the clay combined with the yield stress function has a large effect on the penetration depth and the rebound effect of the clay. This is as such not surprising, however, it was clear that the elastic moduli, 4.136 MPa and 6.58 MPa, used in the two ARL reports by Pamukcu and coworkers [2, 3] together with the yield stress curves presented in the same reports, did not reproduce the experimental results. In order to be able to get close to the experimental results the value of the elastic modulus has to be lowered to 1 MPa or 2 MPa and a damping term had to be added. A value of 1.012 MPa for E was actually used in another study[6]. However, it is clear that the initial approach with a simpler material model for the clay does not allow for a reasonable drop test result.

The use of the *MAT_VISCO_PLASTIC model in IMPETUS, where damping is included, gives much better results, especially, at times after the initial penetration. This model allows the oscillatory behaviour of the clay te be removed by the damping terms. The simulation results that resembled the experiments the most, VP3 and VP5, was with yield stress curves for the clay that was somewhat lower than the experimental results for remolded clay[2]. VP3 matches the yield stress curve for remolded and heated (41° C) clay while the curve for VP5 is between the yield stress curve for remolded clay and remolded and heated clay, see Figures 3.10 and 3.6. The damping terms required for VP3 and VP5 to match the experimental drop tests are very similar. Since the clay used in the ballistic lab at FFI is not heated, the VP5 model parameters were chosen as the model for use in the more complex impact simulations with ceramic and hard steel core projectiles. Despite the small differences in the penetration curves for VP5 and the experimental curves, the model should be more than adequate for further use.

5   Ideas for future work

In this work the position of the clay beneath the steel ball during impact has been compared to the experimental results. A more in-depth study of the clay should test the clay model against more experimental results, such as the permanent clay surface deformation after impact and, if possible, the position (height) in time of a point in the clay a short distance away from the steel impact zone. This would allow for at better in-depth study of the plasticity and elasticity of the clay material model.

Although the visco-plastic material model with parameters from VP5, reproduces the experimental results rather well, it would be interesting to study the strain rate effects of the model. This will give a better idea of whether the model is useful at the higher strain rates that occurs in projectile impact. This does, however, require further experiments as well.

Moreover, it would be interesting to study the effects of changing the clay-mesh used in the simulations. This would give information on whether acceptable results can be obtained with fewer elements and if the results presented above are found with an acceptable mesh size. When the clay model is used in the more complex simulations, like projectile impact, it might be necessary to reduce the number of clay elements to lower the computation time.

Another effect that should be tested is whether the size of the clay box has a huge influence on the results. The reason for this is that the clay box at FFI has a different size than the clay box used at SRI International, with whom the projectile impact experiments are being performed and compared.

Finally, the material model used in other studies of clay, the Drucker Prager model, could be interesting to try. It might be possible to use the *MAT_GRANULAR_CAP model in IMPETUS Afea for this purpose. However, for the time being the results presented in the present work, should be adequate for most simulations, since due to the quality of especially the ceramic models, but also the models for hardened steel.

References

[1] Carlos Ismael Medina. *Dynamic Response of Oily Clay to Impact Loading*. PhD thesis, Lehigh University, 2011.

[2] Sibel Pamukcu, Clay Naiyo, Mesut Pervizpour, Qingsong Cui, Patrick A. Trasborg, Carlos Medina, and Mark A. Mentzer. Distributed fiber-optic sensing and numerical simulation of shock wave response of manufactured clay - phase i: Software model. Technical Report ARL-TR-6399, Army Research Laboratory, 2013.

[3] Sibel Pamukcu, Clay Naiyo, Mesut Pervizpour, Qingsong Cui, Patrick A. Trasborg, Carlos Medina, and Mark A. Mentzer. Distributed fiber-optic sensing and numerical simulation of shock wave response of manufactured clay - phase ii: Software model and breadboard. Technical Report ARL-TR-6400, Army Research Laboratory, 2013.

[4] NIJ. Ballistic resistance of personal body armor - NIJ standard - 0101.06. Technical report, National Institute of Justice, 2008.

[5] T Børvik, OS Hopperstad, T Berstad, and M Langseth. A computational model of viscoplasticity and ductile damage for impact and penetration. *European Journal of Mechanics A - Solids*, 20(5):685–712, 2001.

[6] R Munusamy and DC Barton. Behaviour of roma plastilina upon blunt projectile impact. In *DYMAT 2009 - 9th International Conference on the Mechanical and Physical Behaviour of Materials Under Dynamic Loading*, volume 1, 2009.

[7] *IMPETUS Afea solver - User guide & Keyword manual*, September 2014. URL `http://manual.impetus-afea.com/solver/version/3.0b/overview`.

[8] *IMPETUS Afea solver notes*, July 2014. URL `http://files.impetus-afea.com/download/file/lars/impetus_afea_solver_july_2014.pdf`.

Appendix A Material models for clay

In this work two material models have been used to model the clay. These are described briefly below.

The modified Johnson-Cook model

The *MAT_METAL keyword in IMPETUS is very close to the modified Johnson-Cook material model[5], where the yield stress curve of the material is given by

$$\sigma_y = [A + B\epsilon^n] \, [1 + \dot{\epsilon}^*]^C \, [1 - T^{*m}] \, . \tag{A.1}$$

A, B, n, C and m are material parameters, while ϵ is the strain. $\dot{\epsilon}^* = \dot{\epsilon}/\dot{\epsilon}_0$, where $\dot{\epsilon}$ is the strain rate and $\dot{\epsilon}_0$ a reference strain rate. $T^* = (T - T_{\mathrm{r}}) / (T_{\mathrm{m}} - T_{\mathrm{r}})$, with T being the absolute temperature, T_{r} the reference temperature and T_{m} the melting temperature.

This model is designed for ductile metals and is widely used. In the *MAT_METAL in IMPETUS the yield stress curve can be adjusted by the user, as the $[A + B\epsilon^n]$ term is replaced by a user defined curve σ_ϵ

$$\sigma_y = \sigma_\epsilon \, [1 + \dot{\epsilon}^*]^C \, [1 - T^{*m}] \, . \tag{A.2}$$

Besides this change in the yield stress curve, there are other user definable options in the keyword. These are, however, not relevant for the current work.

The model above can be simplified further by assuming that there is no thermal softening in the clay ($T^* = 0$). With the results by Pamukcu and co-workers in mind[2], this may be a crude assumption. However, the energy in the ball drop is quite low, so the assumption, that there is no appreciable temperature change in the impact event might be reasonable.

Moreover, by setting $C = 0$ the strain rate dependence can be taken out of the equation. This is also a rough assumption, however, it does ensure that the results from the simulations are not due to a strain rate effect, which could prove problematic when using the model in simulations with much larger strain rates. Thus, the yield stress curve boils down to a simple user defined curve

$$\sigma_y = \sigma_\epsilon. \tag{A.3}$$

IMPETUS visco-plastic model

The *MAT_VISCO_PLASTIC material is, as the name suggests, a model which includes both plasticity and a viscosity[7, 8]. The stress in the material model is defined as the sum of three terms. A non-linear viscous stress component, σ_1, a term to define non-linear elastic stress, σ_2 and a linear elastic stress component, σ_3.

$$\sigma = \sigma_1 + \sigma_2 + \sigma_3. \tag{A.4}$$

The non-linear viscous term

The non-linear viscous stress component is given by

$$\sigma_1 = f\left(\dot{\bar{\epsilon}}, \epsilon\right) \cdot \dot{\bar{\epsilon}}\left(t\right). \tag{A.5}$$

This stress component depends on the velocity with which deformation occurs, essentially strain rate, and some curve or function, f, that is dependent on the viscosity of the material. In IMPETUS the strain dependence has been implemented by the term, $\dot{\bar{\epsilon}}$, which can depend on the strain rate for some time before the actual time step. This history dependent strain rate is given by

$$\dot{\bar{\epsilon}}\left(t\right) = \frac{1}{c_{dec}} \int_0^t \dot{\epsilon}\left(\tau\right) e^{(-\tau/c_{dec})} d\tau, \tag{A.6}$$

where $\dot{\epsilon}$ is the actual strain rate, c_{dec} is the strain rate decay constant. As c_{dec} approaches 0, $\dot{\bar{\epsilon}}$ approaches $\dot{\epsilon}$.

The non-linear elastic term

This stress component depends quadratically on the total deviatoric strain, ϵ_{dev},

$$\sigma_2 = 2\alpha G \sqrt{\frac{2}{3}\epsilon_{ij}^{dev}\epsilon_{ij}^{dev}} \cdot \epsilon_{dev}. \tag{A.7}$$

α is a constant that determines the contribution of the non-linear elasticity and G is the shear modulus. The non-linear stress component is particularly interesting for materials that can undergo large elastic deformations without plastic deformation, such as rubber.

The linear elastic term

The elastic term is dependent on the hydrostatic pressure, p, and the deviatoric part of the elastic strain tensor, ϵ_{dev}^e,

$$\sigma_3 = -p\mathbf{I} + 2G\epsilon_{dev}^e. \tag{A.8}$$

The plastic yield stress of this component is given by

$$\sigma_y = \left[\sigma_0 + \sum_2^{i=1} Q_i\left(1 - e^{-C_i\epsilon_{eff}^p}\right)\right] \cdot \left[1 - \left(\frac{T - T_0}{T_m - T}\right)^m\right] \cdot \left[1 + \frac{\beta p}{\sigma_0}\right]. \tag{A.9}$$

The first set of brackets defines the shape of the yield stress curve, with σ_0 as the initial yield stress at zero strain. The terms in the sum, Q_i and C_i, define the shape of the curve. C_i determine how fast the yield stress increases with increasing strain up to the maximum yield stress given by the sum of the pre-factors Q_i and σ_0. The second bracket allows

for a temperature dependence. This is the same as for the Johnson-Cook model, where the yield stress becomes smaller with increasing temperatures, with T_0 being the reference temperature and T_m the melting point. The last bracket allows for the material to be dependent a pressure. The pre-factor β determines the degree of pressure dependence.

For the simulations in this work, the temperature dependence was assumed to be negligible, by the same arguments as presented in Appendix Appendix A. Moreover, to keep the number of a variables to a minimum, the pressure dependence was omitted by setting $\beta = 0$. The yield stress curve is then given by

$$\sigma_y = \left[\sigma_0 + \sum_2^{i=1} Q_i \left(1 - e^{-C_i \epsilon_{eff}^p} \right) \right].$$

(A.10)